

Estimating Aboveground Biomass in Interior Alaska with Landsat Data and Field Measurements

Lei Ji^a, Bruce K. Wylie^b, Dana R. Nossow^c, Birgit Peterson^a, Mark P. Waldrop^d, Teresa N. Hollingsworth^e, Jennifer Rover^b

^aASRC Research and Technology Solutions, contractor to the U.S. Geological Survey (USGS) Earth Resources Observation and Science (EROS) Center, Sioux Falls, SD 57198-0001, work performed under USGS contract 08HQCN007, lj@usgs.gov, ^bUSGS EROS Center, Sioux Falls, SD 57198-0001, wylie@usgs.gov, jrover@usgs.gov,

^cBoreal Ecology Cooperative Research Unit, University of Alaska Fairbanks, Fairbanks, AK 99775-6780, drossow@alaska.edu, ^dUSGS, Menlo Park CA, 94025, mwaldrop@usgs.gov, ^eBoreal Ecology Cooperative Research Unit, Pacific Northwest Research Station, USDA Forest Service, Fairbanks, AK 99775-6780, inhollingsworth@alaska.edu

I. Introduction

Alaska's ecosystems play important roles in the investigation of global climatic change because of the area's extreme environments (e.g., limited sunlight, low temperature, and short growing season), its strong response to global warming (e.g., thawing of permafrost and melting of ice masses), and its representative ecological functions within the global system. Terrestrial biomass is a key biophysical parameter in the studies of Alaska's ecosystems and their response to global warming. However, there is a lack of detailed biomass estimates for this vast and remote region. Our research objective is to produce a 30-m resolution aboveground biomass (AGB) dataset for the Yukon River Basin of Alaska and Canada using Landsat data and field observations acquired in recent years. The AGB estimates for the Yukon Flats Ecoregion in this study is a prototype of regional AGB mapping for the entire basin.

II. Study Area

The Yukon Flats Ecoregion is a relatively flat, marshy basin. The Yukon River and several smaller rivers running through the area, and numerous river tributaries, lakes, and ponds are distributed throughout (Figure 1). According to 2001 the National Land Cover Database (NLCD 2001), the major land cover types are deciduous forest (20.5%), evergreen forest (36.2%), mixed forest (9.1%), shrubs, scrubs, and grasslands (10.8%), woody and emergent herbaceous wetlands (15.0%), and open water (6.4%). Wildfires are very common in the ecoregion. Figure 2 shows the typical vegetation communities in the ecoregion.

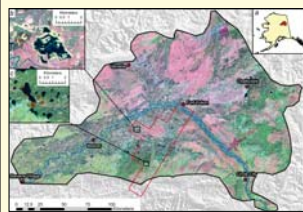


Figure 1. Map of the Yukon Flats Ecoregion showing the Landsat TM images mosaicked from six scenes. The red polygon outlines the airborne lidar extent. (a) The location of the Yukon Flats Ecoregion in Alaska. (b) and (c) Field plots near Canvasback Lake and Boot Lake. The orange points indicate the field sampling sites.



Figure 2. Photographs showing the typical vegetation communities in the study area. (a) White spruce (*Picea glauca*). (b) Black spruce (*Picea mariana*). (c) Quaking aspen (*Populus tremuloides*). (d) Willow (*Salix* spp.). (e) Mixed white spruce and deciduous forest. (f) Water sedge (*Carex aquatilis*). (g) Moss. (h) A recently burned forest.

III. Data

1. Landsat TM data

We selected six cloud-free Landsat 5 Thematic Mapper (TM) scenes acquired from 21 August to 1 September 2008 covering the entire Yukon Flats Ecoregion (Figure 1). We converted the original digital number data to at-sensor reflectance and land surface temperature (LST). A linear regression technique was used to match adjacent scenes, resulting in normalized at-sensor reflectance images.

2. Airborne lidar data

A lidar dataset was collected for an area in the south-central part of the ecoregion in mid-July and early September 2009 (Figure 1). The data products were acquired with an aircraft-carried Optec ALTM Gemini system operated by Aero-Metric, Inc. The company processed the raw data and delivered the 2.5-m raster dataset of bare-earth digital surface model (DSM) and first-return DSM.

3. Field measurements

We preselected 22 sampling sites based on land surface characteristics observed from satellite images and other geospatial data. These were the factors we considered in the site selection: (1) land cover type, (2) vegetation density, (3) walking distance from the base camp to the sites, and (4) public domain. A field campaign was carried out in the areas near Boot Lake and Canvasback Lake from late August to early September 2009. The AGB measured in the field consisted of tree and shrub biomass, coarse woody debris (CWD) biomass, and understory biomass.

IV. Methods

1. Calculation of field aboveground biomass

In this study, total AGB was defined as the sum of tree and shrub (live and dead), CWD, and understory AGB. We estimated tree and shrub AGB (> 1 m) using the diameter at breast height (DBH) or basal diameter (BD), following the allometric equations compiled for interior Alaska. For dead trees and shrubs, the foliage component was subtracted from the total AGB. We sampled CWD with a line intersect method. For each field plot, the sampled understory vegetation was dried and then weighed to calculate understory AGB.

2. Regression model development and regional AGB estimation

We used a regression method to estimate AGB based on eight Landsat-derived spectral indices and LST (predictor variables) and field-measured AGB (response variable) at 20 plots (two burned plots from a 2009 fire were excluded). The spectral indices and LST represent the general land surface characteristics: greenness (NDVI, SAVI, GNDVI, and EVI), moisture (NDII, NDII7, NDWI, and NDWI7), and temperature (LST) (Table 1). However, multicollinearity occurred due to high correlation among the predictor variables in the regression model. Thus, we used a principal component (PC) regression method, where the original predictor variables were linearly transformed to a set of jointly uncorrelated PCs. In general, AGB demonstrated a logarithmic rate of increase against spectral indices and major PCs. To linearize this relationship, we used a logarithmic transformation that converted the AGB to a natural logarithmic form. We used averaged pixel values from a 30x30-m window in the Landsat image. The final regression model was applied to the PC images to generate a map of total AGB for the Yukon Flats Ecoregion.

3. Validation of the AGB models and maps

Because of the small number of field plots, we applied leave-one-out cross-validation (LOOCV) to evaluate the accuracies of the regression model and the AGB map. The mean absolute error (MAE), relative MAE (MAE_r), mean bias error (MBE), and relative MBE (MBE_r) were used to compare the field-measured and model-estimated AGB values. To further assess the accuracy of the AGB map, we used lidar image as an independent validation dataset. The vegetation height was calculated by the difference of the bare-earth DSM data and the first-return DSM data.

Table 1. Landsat-derived spectral indices used to estimate AGB

Index	Equation
Normalized difference vegetation index (NDVI)	$(b4-b3)/(b4+b3)$
Soil adjusted vegetation (SAVI)	$(1+L)(b4-b3)/(b4+b3+L)$
Green NDVI (GNDVI)	$(b4-b2)/(b4+b2)$
Enhanced vegetation index (EVI)	$G(b4-b3)/(b4+C b3-C b1+L)$
Normalized difference infrared index (NDII, NDII7)	$(b4-b5)/(b4+b7)$
Normalized difference water index (NDWI, NDWI7)	$(b2-b5)/(b2+b7)$

To match the resolution of the AGB map, we converted the lidar-derived 2.5-m vegetation height map to 30-m pixel size with a spatial-mean method. Because the lidar data did not detect short understory cover and fallen trees, we compared the lidar-derived products only with the tree and shrub AGB map.

V. Results and Discussion

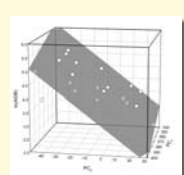


Figure 3. 3-D scatterplot of samples and the best-fit plane surface.

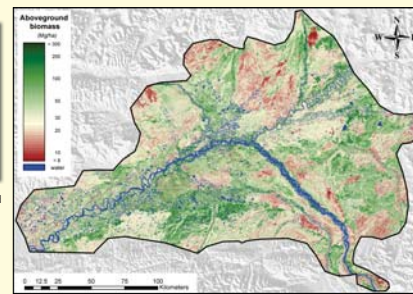


Figure 4. The map of total AGB estimation for the Yukon Flats Ecoregion.

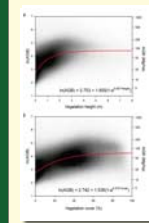


Figure 5. Density scatterplots of AGB estimates vs. lidar-derived vegetation height (a) and cover (b). Red curves indicate exponential regression lines.

1. Regression model and AGB estimation

The final regression model for the regional AGB estimation is

$$\ln(\text{AGB}) = 10.4314 - 0.0185(\text{PC1}) - 0.0411(\text{PC2})$$

The model is significant (p -value < 0.0001) with $R^2 = 0.664$. Figure 3 illustrates a 3-D scatterplot for the 20 plot samples and the best-fit plane surface. This model was applied to the normalized Landsat image mosaic of the Yukon Flats Ecoregion (Figure 1) to estimate the regional $\ln(\text{AGB})$. An exponential equation was then used to transform $\ln(\text{AGB})$ back to total AGB (Figure 4).

Table 2. Leave-one-out cross-validation for the AGB estimation

Metric	Equation	Value
MAE	$(1/n) \sum Y_i - \hat{Y}_i $	35.5 Mg/ha
MAE _r	$(1/n) \sum Y_i - \hat{Y}_i / Y_i \times 100\%$	54.0%
MBE	$(1/n) \sum (Y_i - \hat{Y}_i)$	7.2 Mg/ha
MBE _r	$(1/n) \sum (Y_i - \hat{Y}_i) / Y_i \times 100\%$	16.5%

Note: \hat{Y}_i and Y_i are model-estimated and observed values for sample i .

2. Accuracy assessment

We performed LOOCV for the 20 field plots used for developing the regression model and mapping total AGB (Table 2). For the accuracy assessment with the lidar data, Figure 5 demonstrates the nonlinear relationships between the tree and shrub AGB and lidar vegetation height and cover that we found fit best with an exponential model. The two models were all significant (p -value < 0.0001), with pseudo- R^2 values of 0.392 and 0.366, respectively. We concluded that our total AGB estimates are fairly accurate for the study area.

3. Regional AGB pattern

The AGB frequency chart (Figure 6) shows that the mean AGB value for the study area was 52 Mg/ha and the mode was 24 Mg/ha. Based on the 5% and 95% quantiles, 90% of the study area had AGB values between 13 Mg/ha and 125 Mg/ha. On the AGB map, the spatial AGB pattern primarily follows the distribution of the land cover types. However, most of the low AGB patches correspond with fire events (1986 to 2008) as delineated with Alaska Historical Wildland Fire Perimeters (<http://agdc.usgs.gov/data/blm/fire/>) (Figure 7). The histogram of mean AGB values by land cover type and historical fire burns indicates that the burned areas have relatively low AGB values, implying that fire disturbance is the primary factor that causes the reduction of the regional AGB.

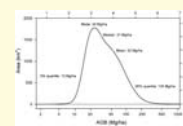


Figure 6. Frequency chart of regional AGB in the Yukon Flats Ecoregion.

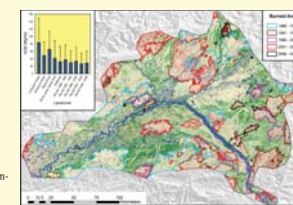


Figure 7. Total AGB estimates overlaid with historical fire perimeters (1986-2008). The insert is the histogram chart of the AGB values by land cover and historical burns.

VI. Conclusions

We completed 30-m resolution AGB mapping for the Yukon Flats Ecoregion using Landsat data and field measurements including tree, shrub, and herbaceous biomass in both live and dead forms. Accuracy assessment of the AGB map indicated that the MAE_r and MBE_r were 54.0% and 16.5%, respectively. We plan to extend the mapping area from the Yukon Flats to the entire Yukon River Basin. We collected additional field biomass data in 2010 in the basin and processed 65 Landsat scenes for wall-to-wall aboveground biomass mapping, which is scheduled to be completed in 2011.

Acknowledgements

This study is funded by the U.S. Geological Survey Climate Effects Network and Global Change Research & Development Programs. We thank Jack McFarland for assistance with field data collection and Jason Stoker for processing the raw lidar data.